Available online at www.sciencedirect.com
SCIENCE DIRECT®
Journal of Sound and Vibration 297 (2006) 329–350
JOURNAL OF SOUND AND VIBRATION
www.elsevier.com/locate/jsvi

Unstable vibration of roller mills

K. Fujita[a,*], T. Saito[b]

[a]Department of Mechanical Engineering, Ube National College of Technology, 2-14-1 Tokiwadai, Ube, Yamaguchi 755-8555, Japan
[b]Department of Applied Medical Engineering Science, Graduate School of Medicine, Yamaguchi University, 2-16-1 Tokiwadai, Ube, Yamaguchi 755-8611, Japan

Received 11 August 2004; received in revised form 17 June 2005; accepted 6 April 2006
Available online 6 June 2006

Abstract

The purpose of this study is to reveal the mechanism of unstable vibration occurring in the grinding operation of roller mills and to show the design guidelines for reducing the vibration. To study the basic cause of the unstable vibration, we first investigated the dynamic characteristics of the mill vibration in its stable state and its unstable state, using a small laboratory roller mill. This showed that the unstable vibration was due to the stick–slip motion of the rollers. Further, the modal analysis showed that the natural frequency of the torsional driving system of the mill corresponded with the unstable vibration frequency. Next, we researched the frictional and compressive characteristics of the ground materials using a simplified test apparatus. This showed that the ground material has a negative-damping property known to be the cause of the self-excited vibration. Furthermore, we proposed the analytical vibration model for the simplified test apparatus considering the negative-damping property, as well as the corresponding equations of motion. By integrating them numerically, fluctuating phenomena similar to the experimental results were obtained.

1. Introduction

A roller mill has several rollers actuated to the rotational table by the hydraulic cylinders and raw materials are ground between the rollers and the table with the assistance of a shearing and compressive force. Over the past 30 years, roller mills have been rapidly employed and widely used to process raw materials in the cement industries because of their superior high efficiency [1–3]. Recently, roller mills have come to be adapted to the grinding of other materials such as ceramic, filler material, etc. due to their power saving capability [4]. However, it has been reported that an unexpected unstable vibration occurred in the course of grinding these materials. This unstable vibration may cause mechanical damage, so the application of roller mills to this region of industry is somewhat hesitant [5].

The unstable vibration of the roller mill is known to be self-excited and to have a fundamental frequency which differs from the frequency inherent to the mill operation. However, so far as conventional research is concerned, very few studies about this unstable vibration have been carried out and the generation mechanism has not been sufficiently clarified [6]. On the other hand, from practical experience, it is well known that the

*Corresponding author. Tel.: +81 836 35 4473; fax: +81 836 22 7801.
E-mail address: katuhide@ube-k.ac.jp (K. Fujita).

0022-460X/$ - see front matter © 2006 Elsevier Ltd. All rights reserved.
doi:10.1016/j.jsv.2006.04.001

unstable vibration is dependent on the fineness of the ground materials. Thus the mill vibration strongly is influenced by the property of the ground materials, while dynamic characteristics of the materials remain unclarified. Therefore, we decided to uncover the mechanism of the unstable vibration occurring in the grinding mills.

In this study, the vibration characteristics of roller mills were researched using a small laboratory roller mill. As a result, it was noted that the unstable vibration was greatly influenced by the behavior of the roller assembly and the stick–slip motion occurring between the roller and the table. In addition, the modal analysis of the roller supporting system and the torsional driving system indicated that the fundamental frequency of the unstable vibration coincides with the first order natural frequency of the torsional driving system. Next, the friction characteristics of the ground materials between the table and the roller were investigated using a simplified test apparatus. As a result, it turned out that the friction coefficient of the ground materials decreased according to the increase of the table speed and this tendency is most marked when fine materials were applied. Further, the analytical vibration model for the simplified test apparatus considering the friction characteristics was proposed and the dynamic formulations were discussed. Finally, the numerical solutions were compared with the experimental results to validate the proposed theoretical analysis.

2. Characteristics of vibration

2.1. Structure of test apparatus

The schematic view of the test apparatus used in this experiment is shown in Fig. 1. The table is directly connected to a gear reducer, and rotated by a motor. The rollers are actuated to the table by hydraulic cylinders through swing levers and rotate depending on the rotation of the table. The raw material, clinker, is fed into the center of the table through a screw feeder then conducted outside the table by the centrifugal force due to the rotation of the table and ground between the rollers and the table. The swing levers can rotate according to the quantity of the material compressed between the table and the roller. The ground materials are then lifted upward, entrained in the air flow, which blows through blade ring provided around the table. The product separator is installed above the grinding portion and classifies the materials into product and return, which goes back to the table.

2.2. Experimental method

The vibration accelerations in the direction of x, y and z are measured on each point as shown in Fig. 1 in the stable state and the unstable state. Further, to grasp the behavior of the roller and the swing lever during the unstable vibration, the rotational motion of the roller and the swing motion of the swing lever are measured. As for the rotational motion of the roller, a shaft with a small rotating device is set into the center of the roller, and the rotational motion of the shaft is measured by a rotary encoder (2500 P/rev) as shown in Fig. 2. As for the swing motion of the swing lever, its up-and-down motion is measured by a laser displacement sensor set on the hydraulic cylinder as shown in Fig. 3.

2.3. Vibration characteristic

The time responses in the x-direction of the point ① and its frequency spectrum in the stable and unstable state are shown in Figs. 4 and 5 respectively. Fig. 5 shows that the fundamental frequency of the vibration in the unstable state is about 47 Hz. Similar results are found for the other points. From now on, the authors will call this unstable vibration "mill vibration" and this fundamental frequency "mill vibration frequency".

The operational condition of the roller mill in this experiment is shown in Table 1. The rotation speed of the table and the rotation speed of the separator have the operational frequency. But the operational frequency does not coincide with the mill vibration frequency, it is thus considered that the mill vibration originates in the natural system of the roller mill. Therefore, the vibration mode of the roller supporting system in the unstable state is investigated by the transfer function between the measured points. In the expression of the vibration mode, the supporting system is modeled by the measured points from ① to ⑩ as shown in Fig. 6. The vibration

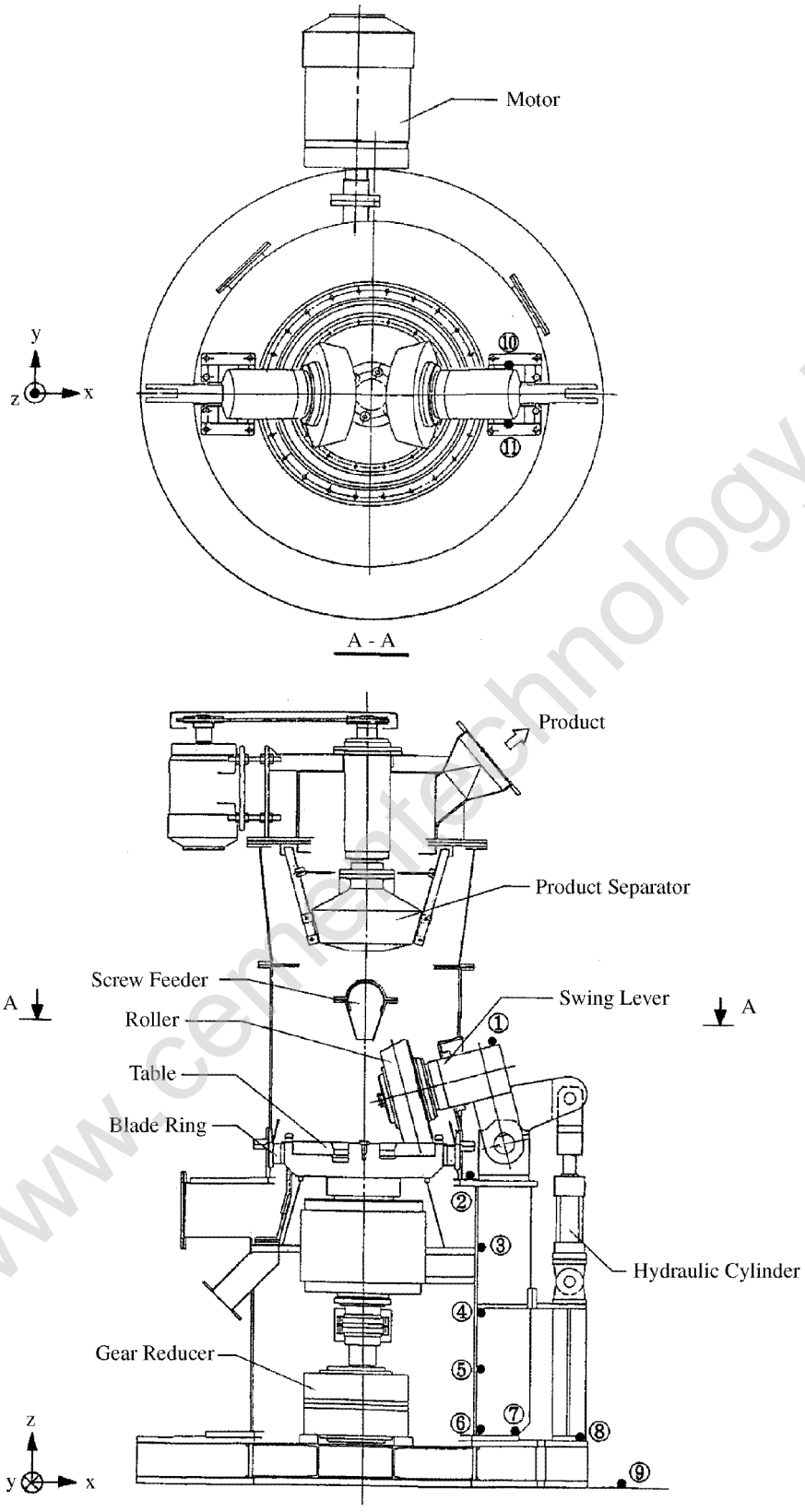

Fig. 1. Test apparatus of roller mill.

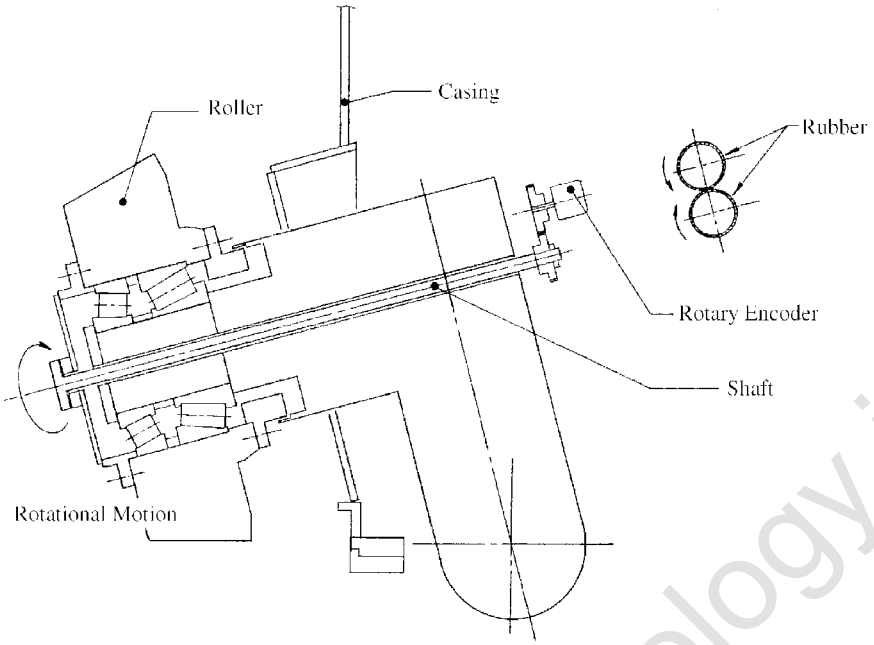

Fig. 2. Measurement method of the rotational motion of the roller.

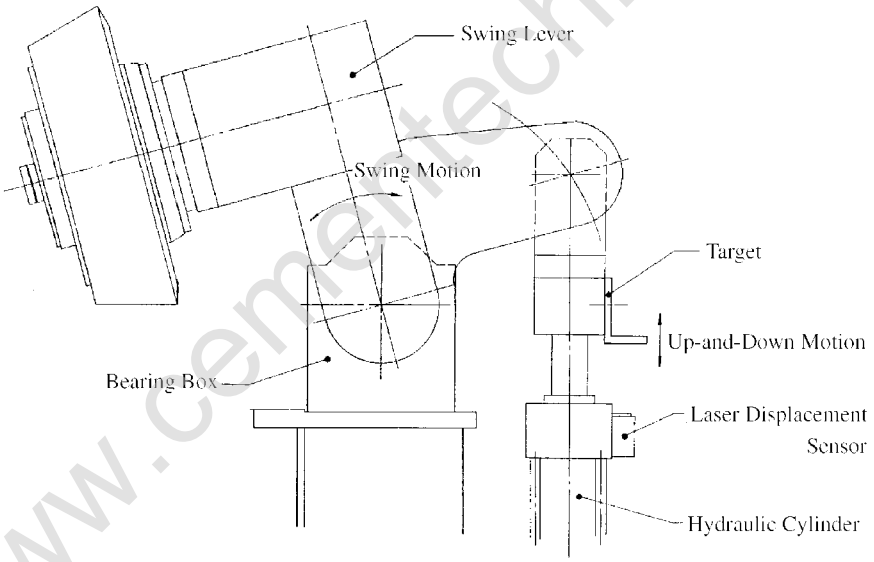

Fig. 3. Measurement method of the swing motion of the swing lever.

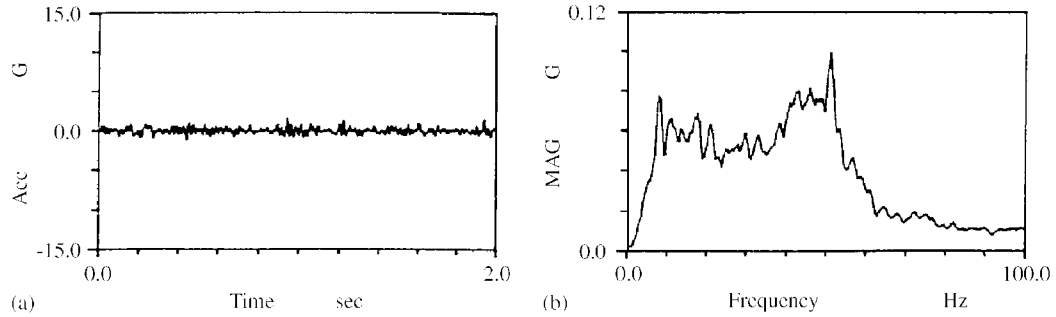

Fig. 4. Vibration characteristic in the stable state: (a) time response; (b) frequency spectrum.

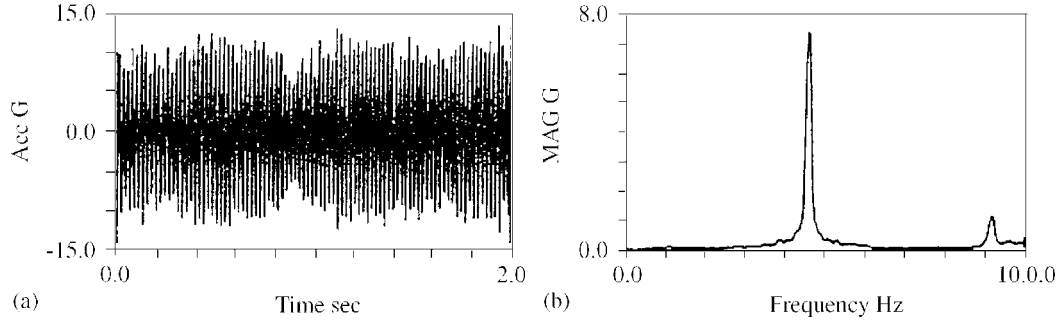

Fig. 5. Vibration characteristic in the unstable state: (a) time response; (b) frequency spectrum.

Table 1
Grinding condition of the roller mill

	Stable state	Unstable state
Capacity (t/h)	0.5	0.5
Rotation speed of table (rev/min)	74	74
Compressive force of roller (kN)	54	54
Air flow rate (m^3/min)	60	60
Rotation speed of separator (rev/min)	150	300

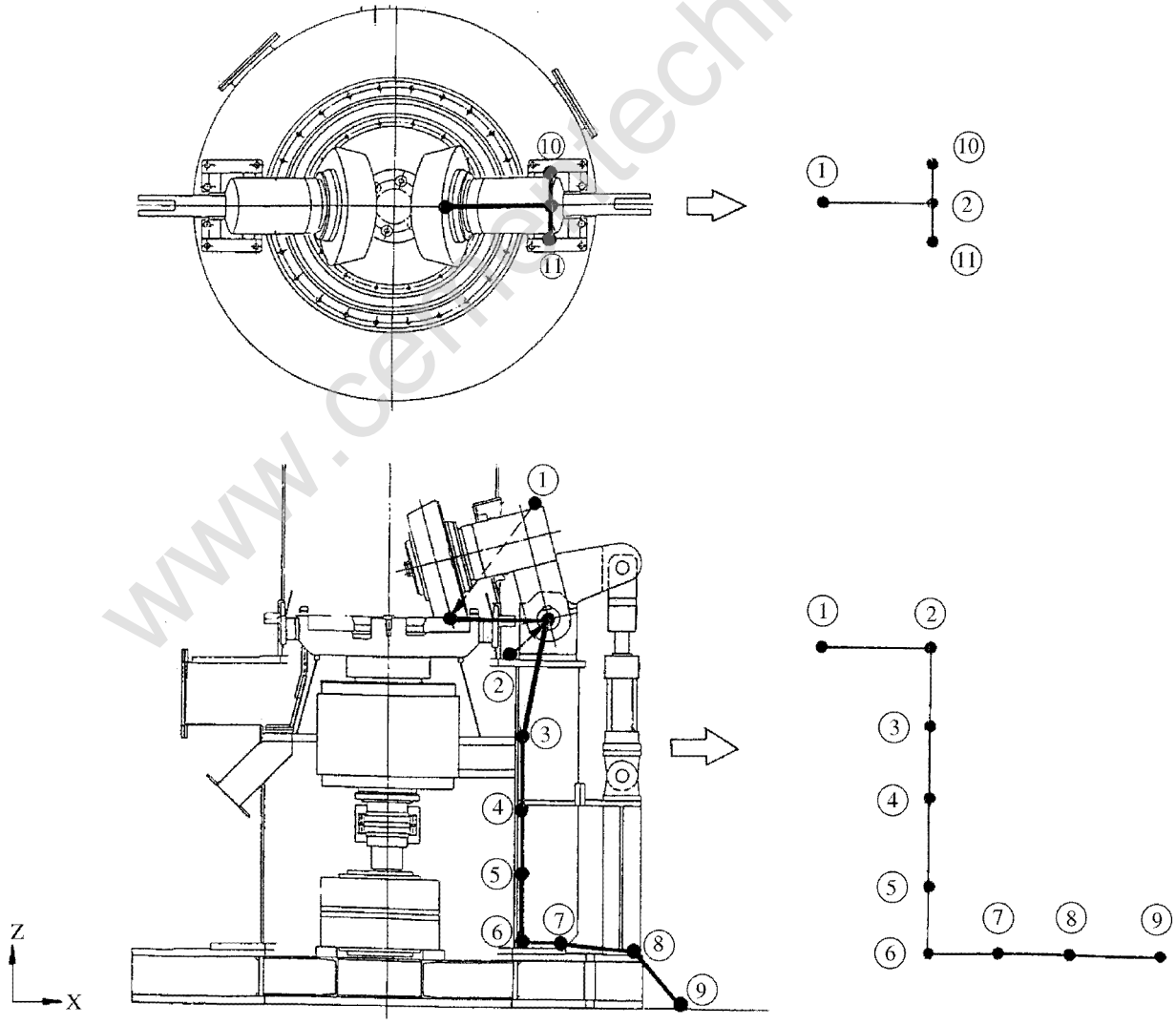

Fig. 6. Mode expression of the roller supporting system.

mode in the unstable state is expressed in Fig. 7. This mode shape shows the normalized maximum amplitude states simultaneously with its quiescent state. It seems that the roller assembly may influence the vibration since the amplitude of the point from ① to ③ is significant compared with the other points.

The rotational motion of the roller and the swing motion of the swing lever in the unstable state are shown in Fig. 8. It shows that when mill vibration occurs, the roller and the swing lever tend to fluctuate with the

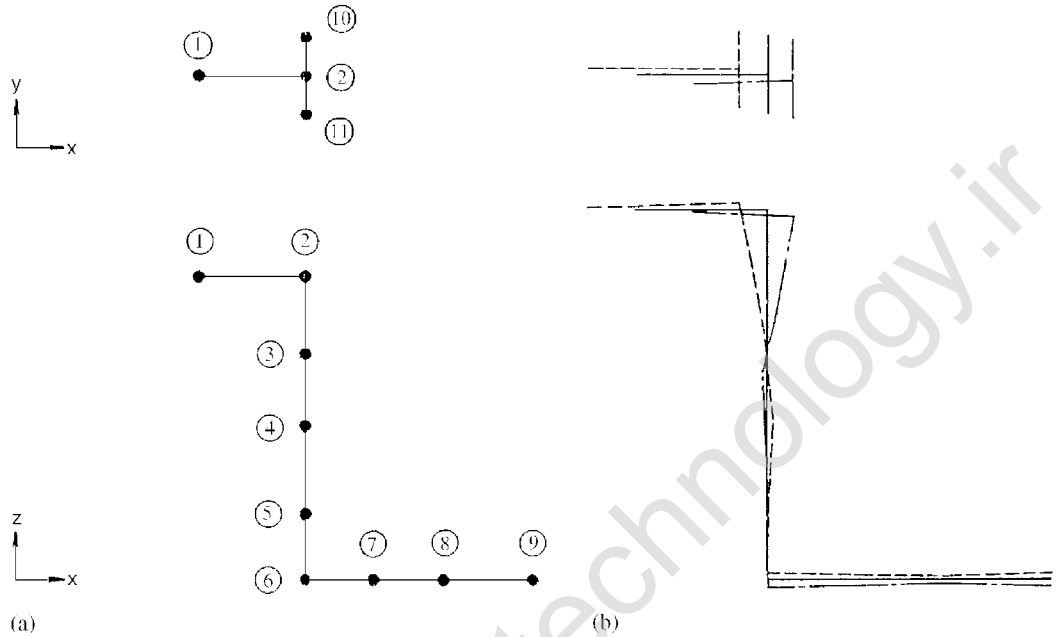

Fig. 7. Vibration mode of the roller supporting system in the unstable state: (a) the model of the roller supporting system and the number indicate the measuring point shown in Fig. 1; (b) solid line quiescence; dotted line the amplitude of the point ① is maximum; speck chain line the amplitude of the point ① is minimum.

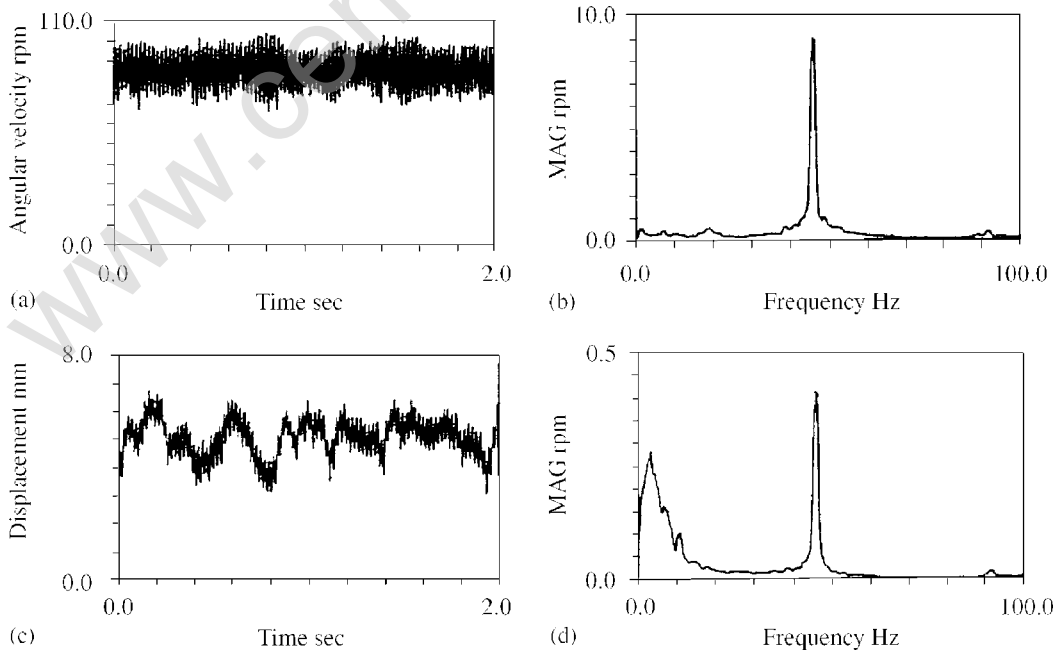

Fig. 8. Motion of roller assembly in the unstable state: (a) time response of the rotational motion of the roller; (b) frequency spectrum of the rotational motion of the roller; (c) time response of the swing motion of the swing lever; and (d) frequency spectrum of the swing motion of the swing lever.

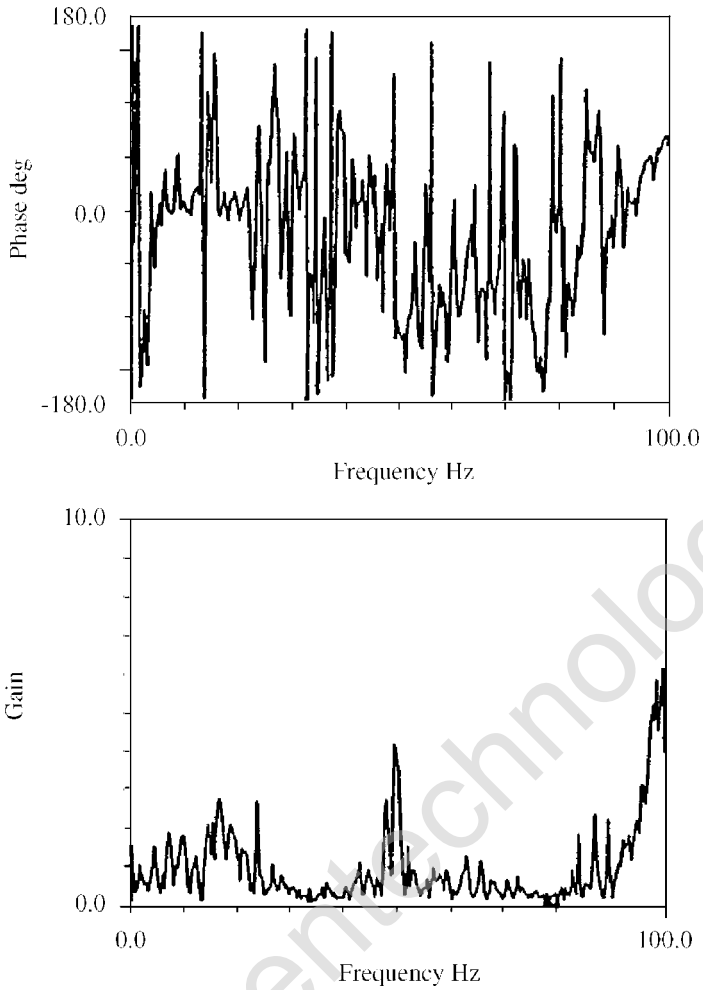

Fig. 9. Transfer function between the angular velocity of the roller and the angular velocity of the table.

same frequency as the mill vibration. So the transfer function, which expresses the ratio of the angular velocity fluctuation of the roller to the angular velocity fluctuation of the table, is analyzed. From the result shown in Fig. 9, it turns out that the gain of the transfer function at 47 Hz is much larger than the ratio of rotational radius of the table to that of the roller (the magnifying ratio is about 1.1). If the roller is rotating without slipping to the table, the gain of the transfer function must be in agreement with the ratio of rotational radius. Therefore, it is considered that the stick–slip motion occurs between the roller and the table.

3. Examination about the natural frequency

As mentioned above, there is no force whose operational frequency coincides with the mill vibration frequency, so the natural frequency of the roller supporting system and the torsional driving system are measured.

3.1. Modal analysis for roller supporting system

Natural frequencies and natural modes are researched by the experiment using the impulsive-force-excitation method. In the impulsive-force-excitation method, we can select the single-point-excitation method or the multiple-point-excitation method. Because of the large structure of this case, the single-point-excitation method cannot activate adequate responses for all points. Therefore, the multiple-point-excitation (① to ⑨) as well as the single-point-response (①) are adopted as shown in Fig. 10. Further, the excitation for the state with the materials laid between the table and the roller is also actuated to estimate the grinding state. The first five

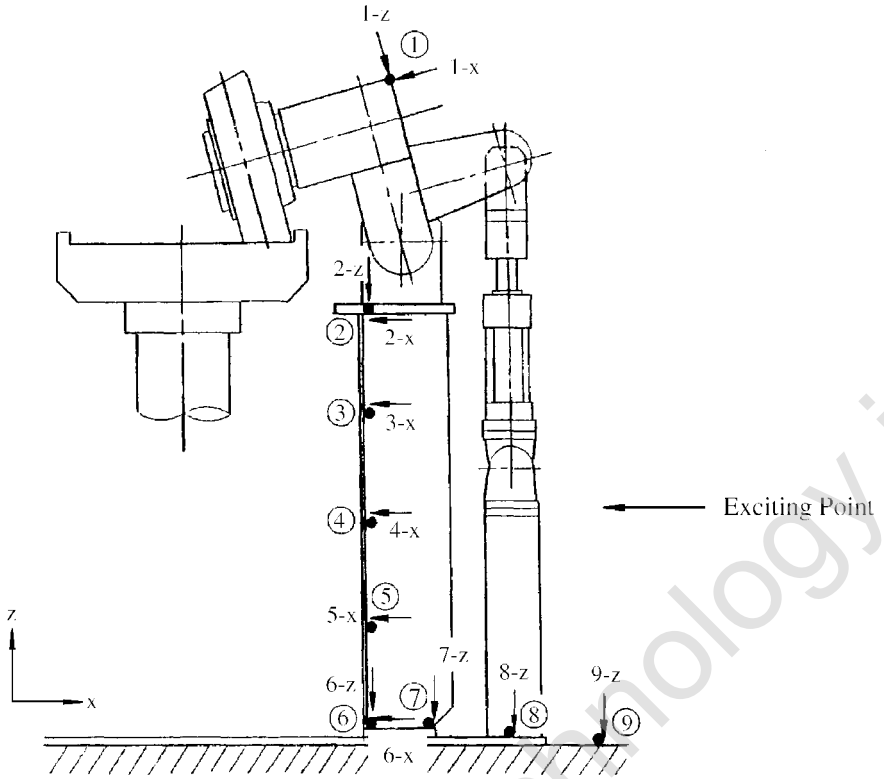

Fig. 10. Exciting points and direction for the roller supporting system.

natural frequencies and natural mode shapes are depicted in Fig. 11. Compared with the mode shapes shown in Fig. 7, the vibration mode in the unstable state is similar to the fourth mode or the fifth mode.

3.2. Modal analysis for torsional driving system

Since the rotational motion of the roller fluctuates with the same frequency as the mill vibration frequency, the spring elements of the driving system rotating the table is considered one of the causes of the mill vibration. So the natural frequency and the natural mode of the driving system are calculated. In this calculation, the torsional driving system is modeled as shown in Fig. 12 and its parameters are shown in Table 2. Parameters, except for J7 and J8, are the catalogued value. J7 for the table and J8 for the roller are calculated from their geometric parameters.

The first three natural frequencies and natural mode shapes are shown in Fig. 13. It can be seen that the first-order natural frequency is about 48 Hz and agrees well with the mill vibration frequency. Therefore, a similar comparison is performed for the production machine with a very large size different from the tested one, and the result is shown in Table 3. It is found that the mill vibration frequency of the actual machine (type A) and the natural frequency of the torsional driving system also shows a good agreement. Observing this result, the driving motor of the actual machine is exchanged for another motor with a small moment of inertia in order to change the natural frequency of the torsional driving system. Under this condition, the vibration of the actual machine is measured. As a result, it is confirmed that mill vibration frequency varies with the change in the natural frequency of the torsional driving system (type B). From these facts, the mill vibration is considered as the vibration originating not from the roller supporting system but from the torsional driving system.

Considering the mechanism of force acting in the torsional driving system, the driving torque by the motor is transferred to the roller by the friction force through the raw materials between the table and the roller, so that the roller is dependently rotated by this friction force. The natural frequency in the torsional driving system agrees with the mill vibration frequency and the stick–slip motion is observed in the rotational motion of the roller caused by the friction force. Because of these results, it is considered that the friction force

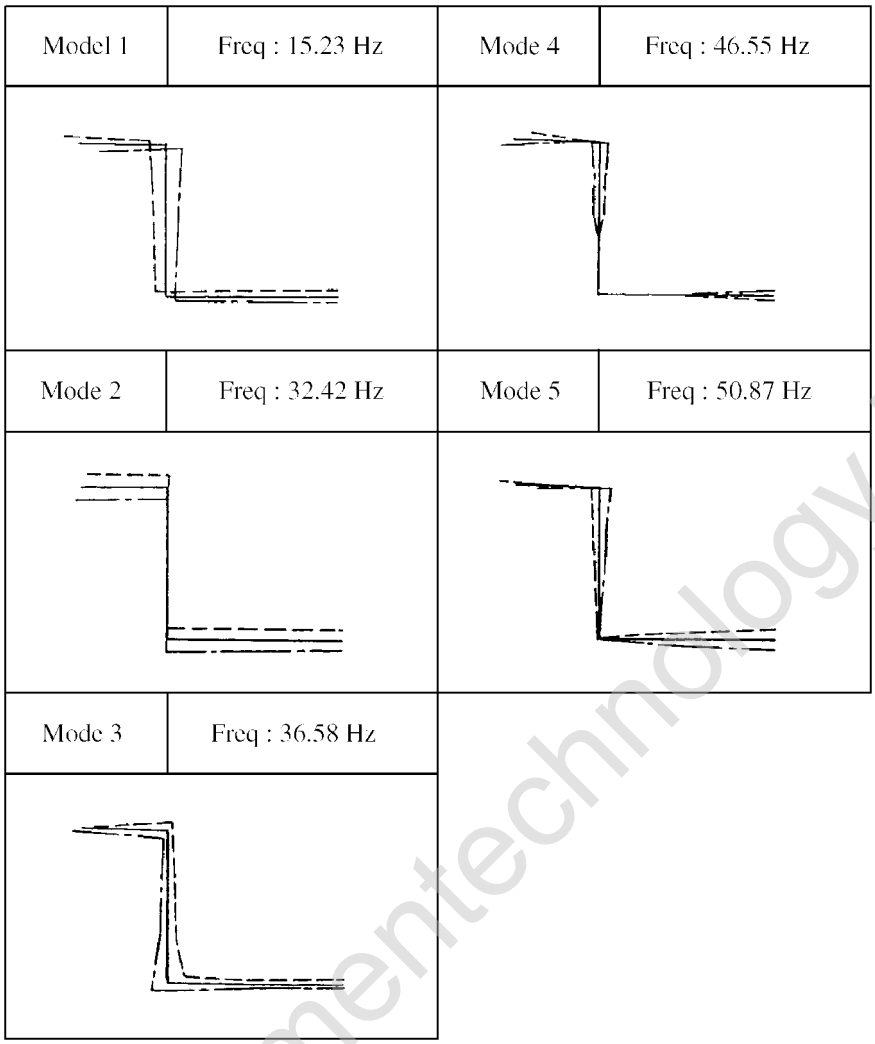

Fig. 11. First five natural frequencies and natural mode shapes for the roller supporting system.

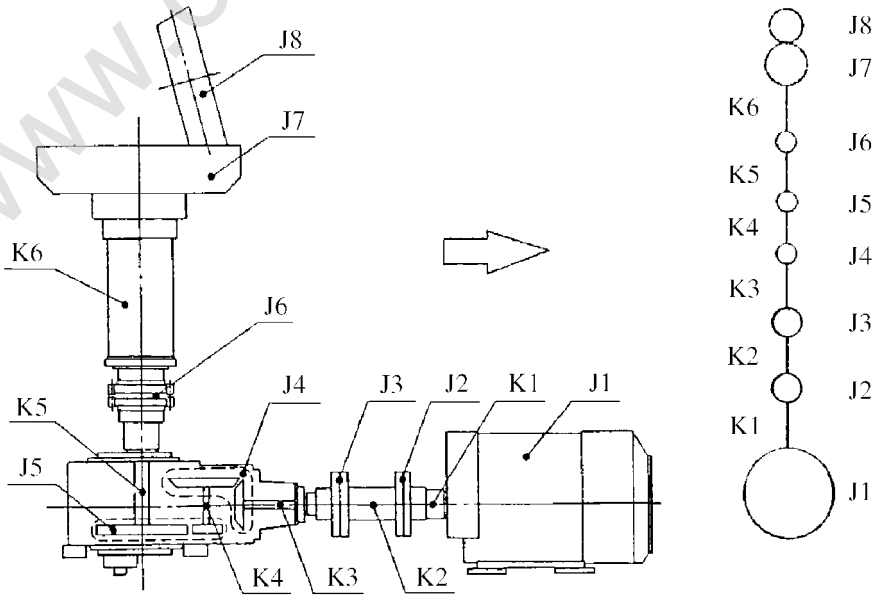

Fig. 12. Modeling of the torsional driving system.

Table 2
Parameters for the torsional driving system

Number	J: Inertia of moment (kg m^2)	K: Torsional stiffness (Nm/rad)
1	7.252	4.096×10^5
2	0.103	5.537×10^4
3	0.105	1.793×10^5
4	0.012	2.117×10^5
5	0.003	6.595×10^4
6	0.005	1.588×10^5
7	0.147	
8	0.048	

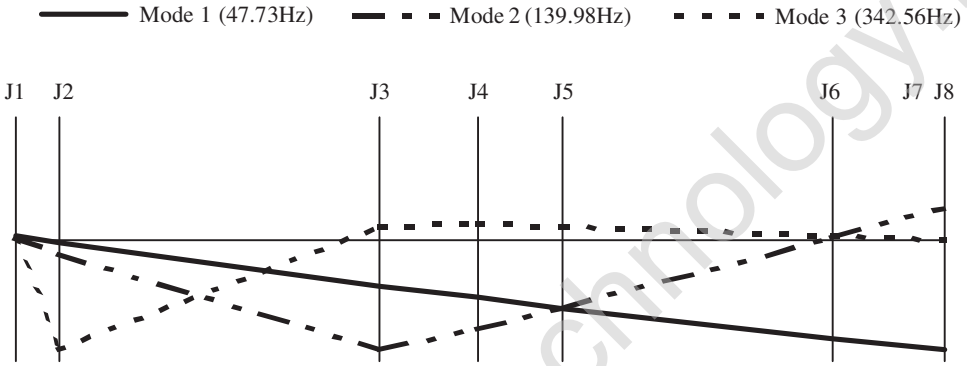

Fig. 13. First three natural frequencies and natural mode shapes of the torsional driving system.

Table 3
Comparison of mill vibration frequency and natural frequency

Type	Vibration frequency (Hz)	Natural frequency (Hz)
	Experiment	Calculation
A	18.8	18.5
B	23.8	23.4

significantly influences the mill vibration. Concerning the vibration in accordance with the friction force, a self-excited vibration with a negative-damping property accompanied by friction is well known [7–9]. So the friction characteristics of materials are measured by a fundamental experiment.

4. Characteristics of materials

4.1. Test apparatus

An outlined structure of the test apparatus is illustrated in Fig. 14. The roller, pressed by hydraulic cylinders, can move in the up-and-down direction, and the table pulled by the motor rotation through the chain can move in the horizontal direction. Further, the table speed can be variably controlled by means of the adjustable speed motor .

4.2. Experimental method

The materials are laid on the table after which the roller is actuated to the table. By pulling the table as it is, the materials are guided and ground between the table and the roller as shown in Fig. 15.

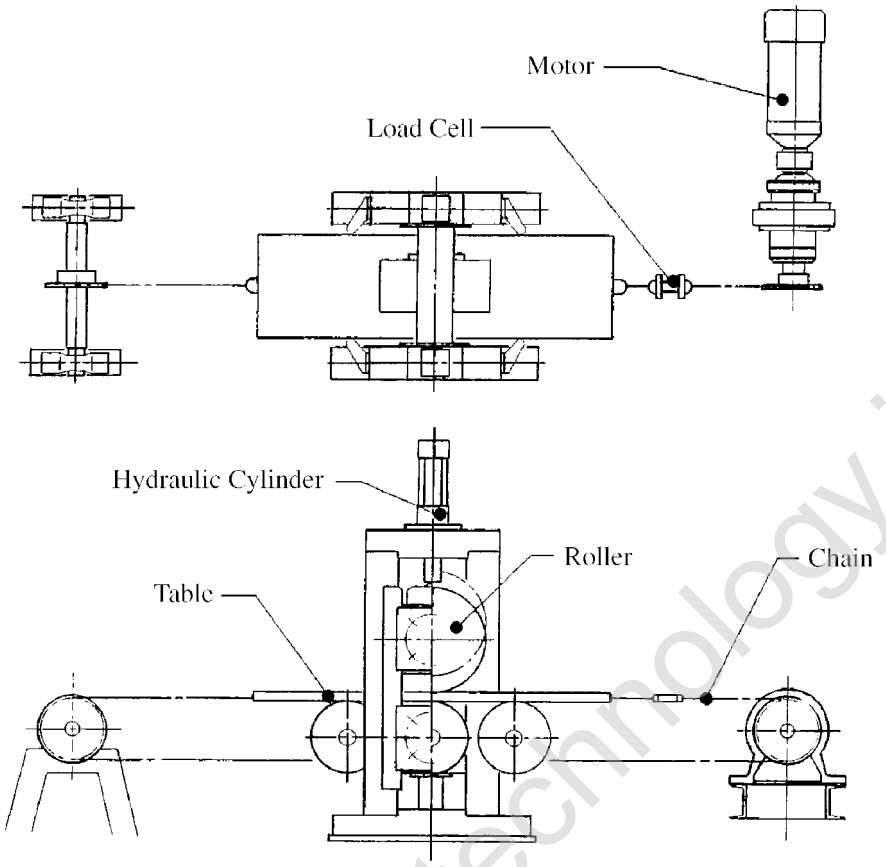

Fig. 14. Test apparatus.

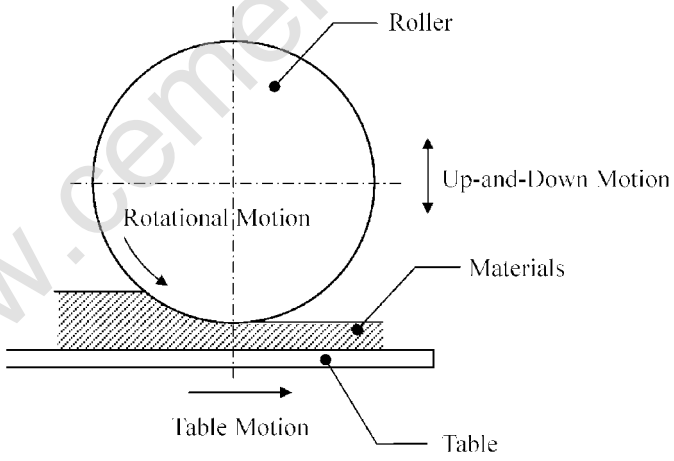

Fig. 15. Schematic diagram of grinding in test apparatus.

In this experiment, the influence of the grain size of the materials, the compressive force of the rollers and the table speed upon the friction characteristics of materials are researched. The measuring instruments are shown in Fig. 16. The compressive force of the roller is measured by a load-cell set under the hydraulic cylinder. The rotational motion of the roller is measured by a rotary encoder directly connected to the rotational shaft. The up-and-down motion of the roller is measured by a laser displacement sensor. Further, the compressive pressure generated in the materials during the grinding operation is measured by the load cell arranged under the table. Here, the compressive pressure is transmitted to the load cell through a pin. So cellophane sheet, whose thickness can be disregarded, is stuck on the table to avoid the penetration of the materials to the pin. The tensile force applied to the table is measured by the load-cell as shown in Fig. 14.

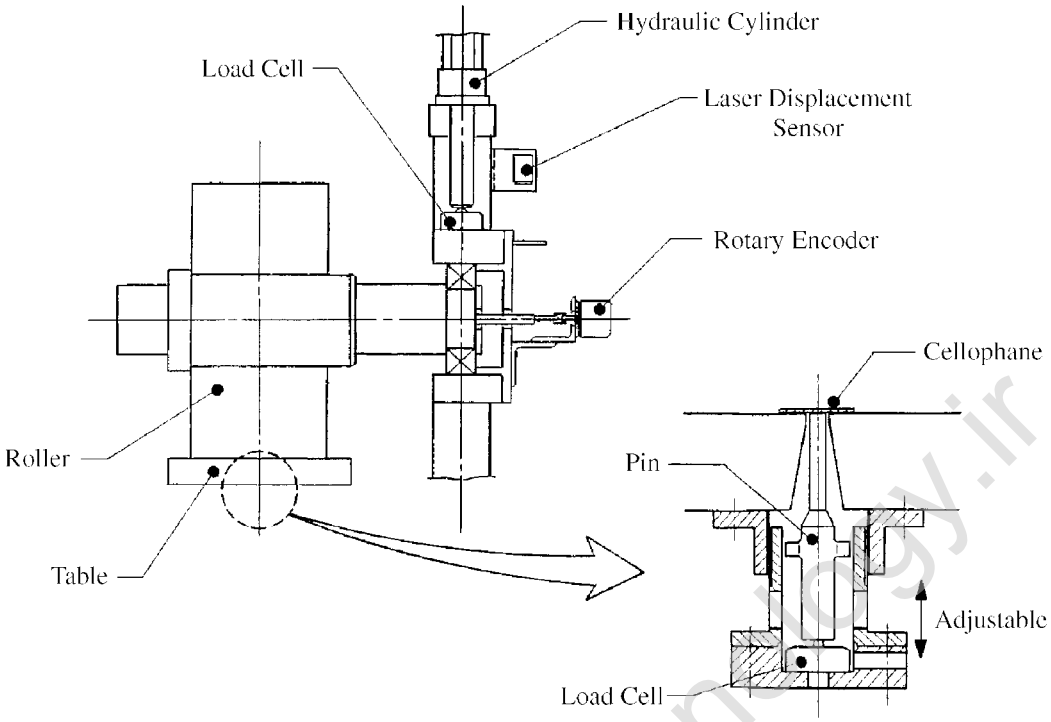

Fig. 16. Measuring instruments of test apparatus.

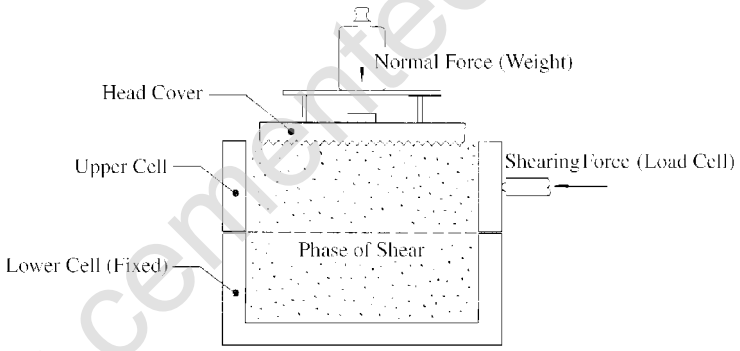

Fig. 17. Direct shearing tester.

The compressive characteristics are evaluated from the pressure distribution of materials between the table and the roller. The kinetic frictional coefficient is evaluated as the ratio of the compressive force of the roller to the tensile force of the table. For comparison, the static frictional coefficient is measured by the direct shearing tester shown in Fig. 17. In the direct shearing tester, the upper cell is pushed very slowly against the lower cell through a load cell. The static friction is evaluated from the relationship between the shearing force when the upper cell begins to move and the normal force.

4.3. Experimental results

Fig. 18 shows the time-response of the compressive force of the roller, the tensile force of the table, the up-and-down motion of the roller, and the angular velocity of the roller respectively. Here, the displacement in Fig. 18(c) shows the thickness of materials between the table and the roller. So the zero value of the displacement corresponds to the state where the roller and the table contact directly with no material in-between.

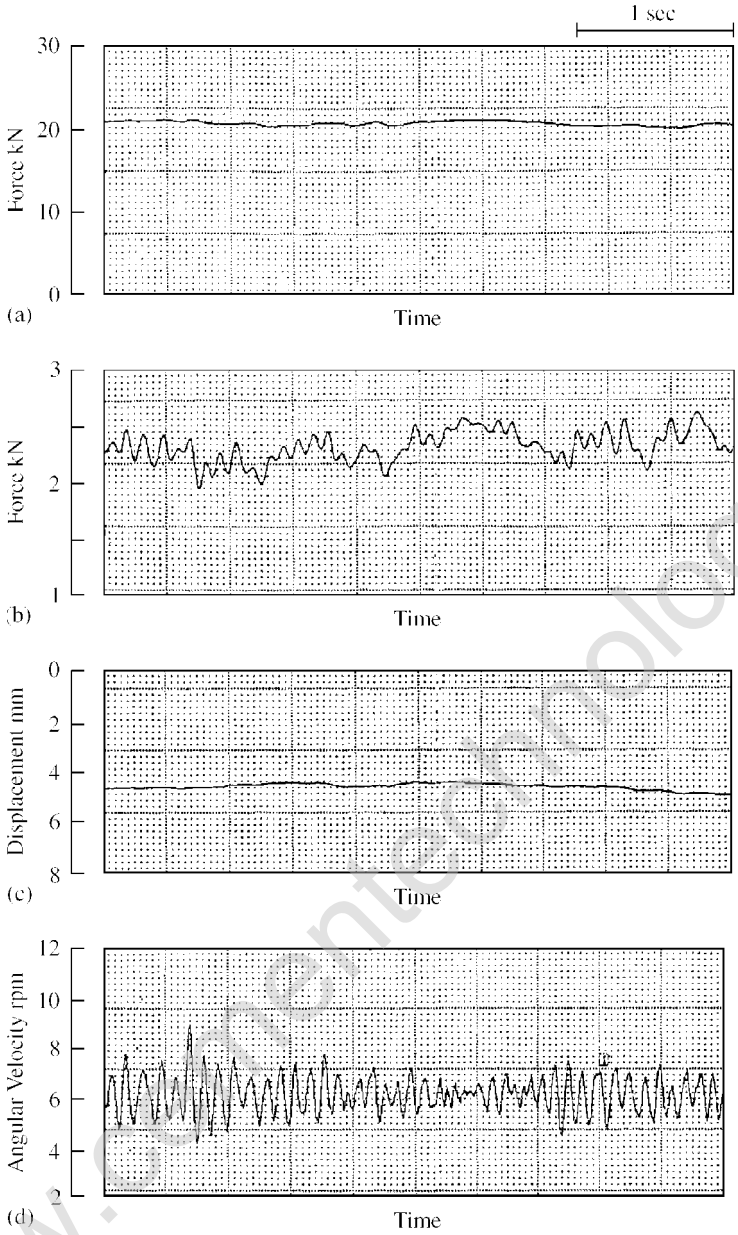

Fig. 18. Experimental results: (a) compressive force of the roller; (b) tensile force of the table; (c) up-and-down motion of the roller and; (d) angular velocity of the roller.

Since the tensile force fluctuates while the compressive force is constant, it is considered that the friction force varies. So the friction coefficient is evaluated from the average ratio of the tensile force to the compressive force. Then the effect of the compressive force and the table speed on the friction coefficient is researched. The characteristics obtained are shown in Figs. 19 and 20. The data plots corresponding to the 0 mm/s speed in Fig. 20 mean the static friction coefficient. Fig. 19 indicates that the compressive force has no effect on the friction coefficient. On the other hand, Fig. 20 shows that the friction coefficient decreases according to the increase in the table speed and its tendency is marked with the fine material.

Then, as shown in Fig. 21, the accelerometer was attached on the table and the fluctuation of the table speed was investigated, and further it was compared with that of the tangential velocity of the roller. From the result shown in Fig. 22, it is observed that the table speed changes at the same frequency as the tangential velocity of the roller. Moreover, the stick state, where the table speed equals the tangential velocity of the roller (as indicated by the dashed line in Fig. 22), and the slip state, where the tangential velocity of the roller is slower than that of the table, takes place alternatively during the fluctuation. This phenomenon means the occurrence

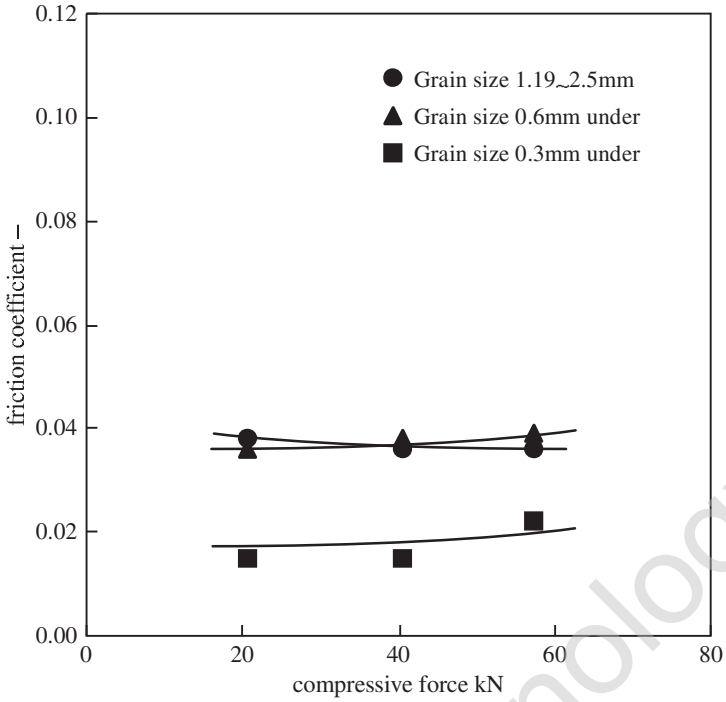

Fig. 19. The effect of compressive force on the friction coefficient under different conditions of grain size of material.

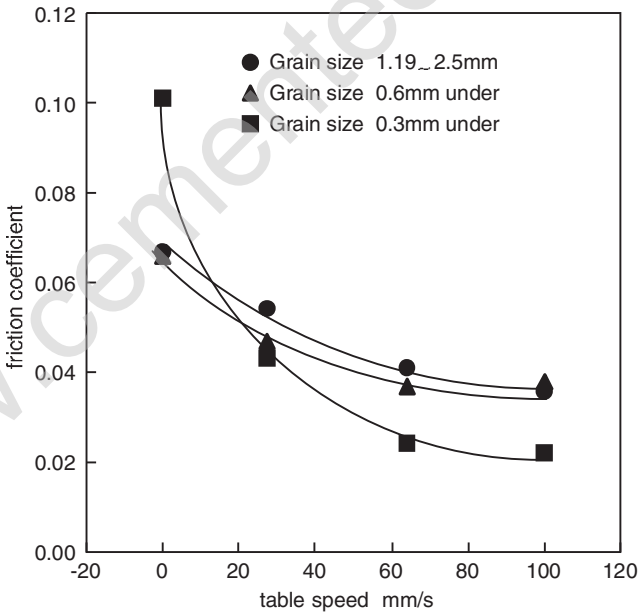

Fig. 20. The effect of table speed on the friction coefficient under different conditions of grain size of material.

of the stick–slip motion between the table and the roller. Further, the frequencies (about 11 Hz) of fluctuation in both the table speed and the tangential velocity of the roller coincide with the natural frequency of the driving system, when it is calculated assuming the chain as a spring element and the roller as an inertia element. This result also agrees with the characteristics of the mill vibration.

The pressure distribution of material relative to the roller position is shown in Fig. 23. It is confirmed that the maximum pressure point exists at the position which is located in the entrance side, a small distance from the lowermost part of the roller, and even after passing the lowermost part of the roller, the pressure remains for a while. The compressive displacement and the compressive force are computed from this pressure

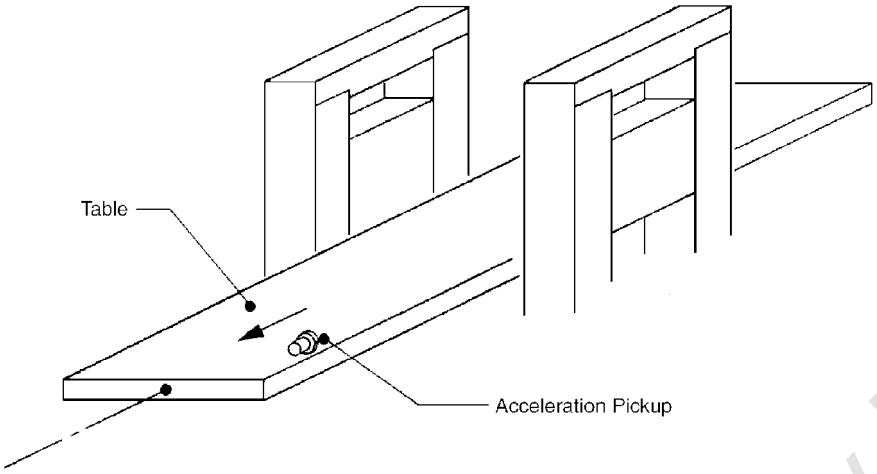

Fig. 21. Measurement method of table speed.

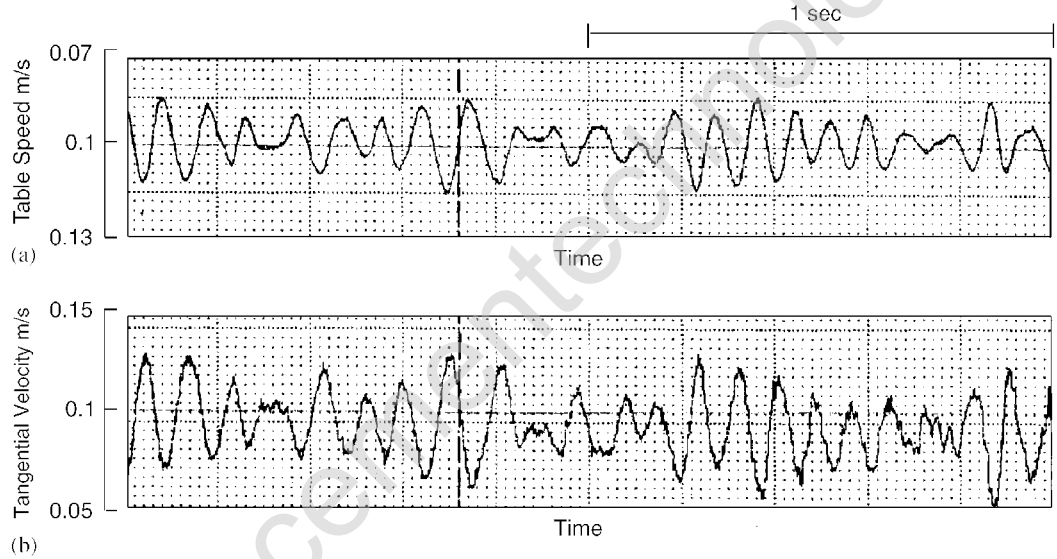

Fig. 22. Relation between the table speed and the tangential velocity of the roller: (a) table speed; and (b) tangential velocity of the roller.

distribution, and from the relationship between the displacement and the force, the compressive characteristics of materials are derived. The compressive characteristics obtained are shown in Fig. 24 together with the approximation curves.

Since the nonlinearity of the compressive characteristics are strong, a suitable approximation can not be obtained by the least-squares method. Thus, the compressive characteristics are estimated via the following formula of the exponential function which agrees comparatively well within the range of this analysis application.

$$F = 1.5 \times \{\exp(\delta) - 1.0\} \quad \text{in the case of coarse materials,}$$
$$F = \begin{cases} 0.0 & (0 \leqslant \delta \leqslant 1.5) \\ 4.5 \times \{\exp(\delta) - 1.0\} & (\delta > 1.5) \end{cases} \quad \text{in the case of fine materials,} \tag{1}$$

where F is the compressive force and δ is the compressive displacement. Also in the compressive characteristics, it is confirmed that nonlinearity becomes marked when the material is finer.

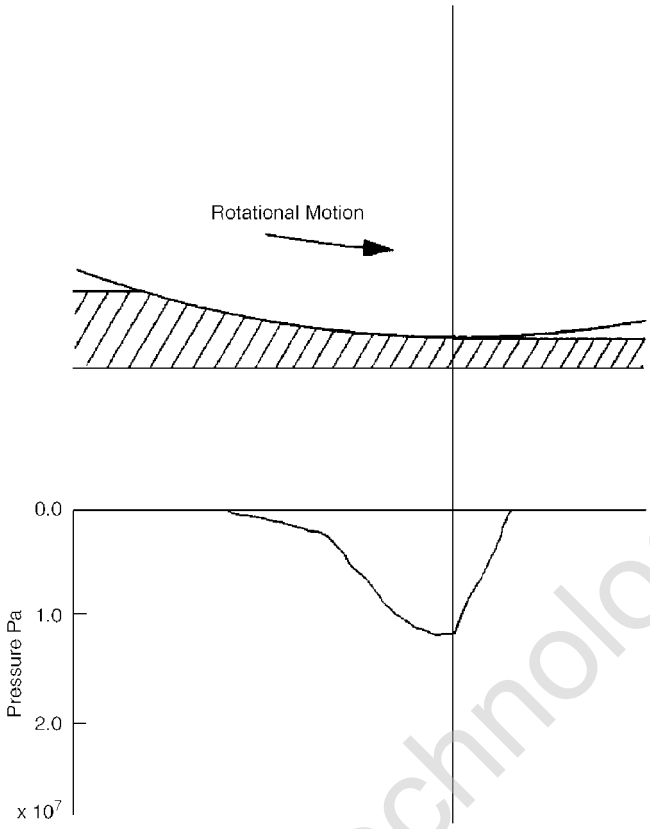

Fig. 23. Pressure distribution of material relative to the roller position.

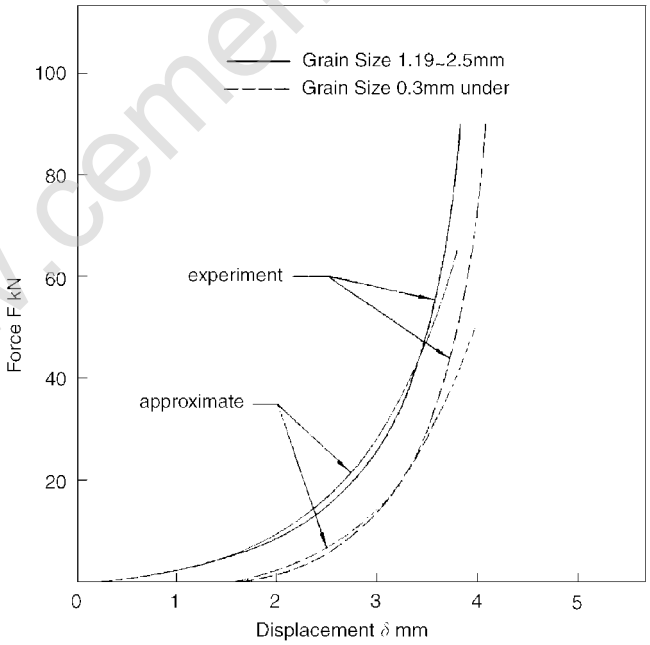

Fig. 24. Compressive characteristics.

It is established that stick–slip motion occurs when the friction force decreases in accordance with the increase of sliding speed or its discontinuous transition takes place from the static state to the kinetic state. As previously mentioned, the grain size of materials has a great influence on the mill vibration and mill vibration occurs with fine material. From these facts, the cause of the mill vibration is considered to be the friction

characteristics of materials, that is, the friction coefficient decreases according to the increase of the table speed, and the mill vibration is due to the stick–slip motion of the roller. So the vibration model, which generates a self-excited fluctuation in the rotational motion of the roller, is proposed, using the compressive characteristics and the frictional characteristics obtained by the experiment.

5. Vibration model

5.1. Force balance of grinding area

In making a vibration model, the force balance of the grinding area is considered. Fig. 25 shows the force balance in the grinding area. The materials of initial thickness H are sent to the grinding area by the movement of the table, and are ground by the compressive force P. The force F_v accompanying the compressive force, acts perpendicularly on the table through the materials, and the reaction force acts on the roller in the opposite direction. For the table, in addition to the force F_v, the tension force T from the chain and frictional force μF_v from materials, act simultaneously. The roller rotates by the frictional force, $\mu F_v \cos\alpha$ while the tangential component of reaction force $F_v \sin\alpha$ acts on the roller in the opposite direction. In practice, the forces which the roller receives from the materials are transmitted through the contact surface of the roller and the materials. In this analysis, the centroid of the pressure distribution is obtained from the computation and its position is defined by the angle α as shown in Fig. 25. The force acting on the roller is transmitted at this point in order to simplify analysis.

5.2. Vibration model

Considering the balance of force as shown in Fig. 25, the test apparatus can be modeled by the three-degrees-of-freedom system as shown in Fig. 26. Namely, the displacement of the table, the up-and-down displacement of the roller and the rotation angle of the roller are expressed with x_1, x_2 and θ_2, respectively. Then equations of motion can be expressed as follows:

$$m_1\ddot{x}_1 = T - \mu F_v, \tag{2}$$

$$m_2\ddot{x}_2 = F_v - (P + m_2 g), \tag{3}$$

$$I_2\ddot{\theta}_2 = r(\mu F_v \cos\alpha - F_v \sin\alpha). \tag{4}$$

As for this system, materials are continuously sent between the table and the roller. In the formulization of the steady state, we consider that the materials are stably sent between the table and the roller and vibration

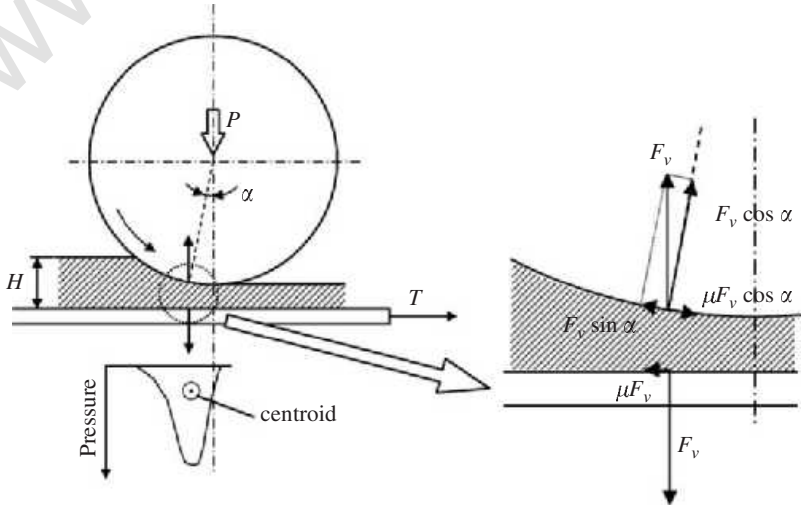

Fig. 25. Force balance in the grinding area.

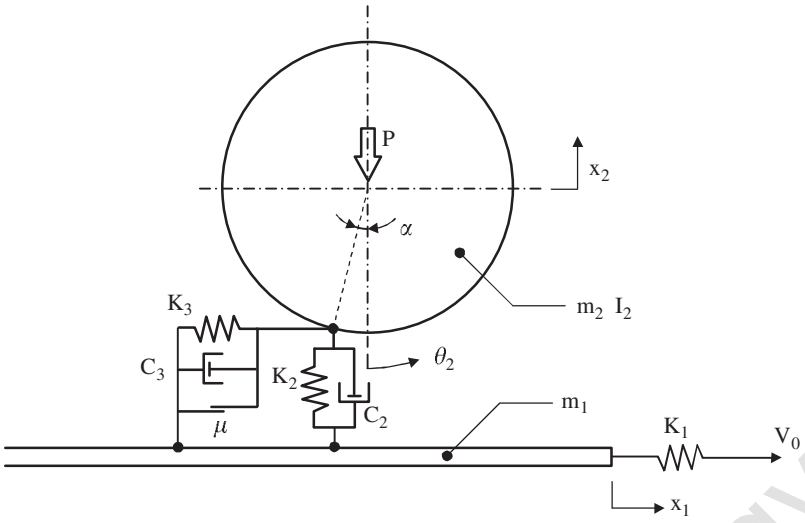

Fig. 26. Vibration model.

never occurs. In the steady state, the tension force T, the perpendicular force F_v and the friction coefficient μ can be written as

$$T = K_1(V_0 t - x_1), \quad F_v = K_2(H - x_2) - C_2\dot{x}_2, \quad \mu = f(\dot{x}_1 - r\dot{\theta}_2). \tag{5}$$

Here, we consider the steady-state constants, K_3 and C_3, for the horizontal direction of materials. Generally, however, the magnitude of the steady-state constants does not affect the balance of force. In this case, it is also difficult to identify the steady-state constants for the horizontal direction, so they are not considered in Eqs. (2)–(4).

Considering the case of the steady-state situation, i.e., $\ddot{x}_1 = \ddot{x}_2 = \ddot{\theta}_2 = 0$, $\dot{x}_1 = V_0$ and $\dot{x}_2 = 0$, the state can be obtained by solving Eqs. (2)–(5)

$$x_1 = V_0 t - \frac{P + m_2 g}{K_1}\tan\alpha, \quad \ddot{x}_1 = V_0, \tag{6}$$

$$x_2 = H - \frac{P + m_2 g}{K_2}, \quad \dot{x}_2 = 0, \tag{7}$$

$$f(V_0 - r\dot{\theta}_2) = \tan\alpha. \tag{8}$$

In the following, we consider the case of the unstable state with disturbance from the steady state. The variables which show the disturbance are defined as s_1, s_2 and ϕ_2 from x_1, x_2 and θ_2 respectively. When the disturbance occurs, it is considered the restoring force and the damping force occur in the materials between the table and the roller. The perpendicular component and the horizontal component of these forces can be calculated as:

$$\text{perpendicular component}: \quad K_2(r\phi_2 \sin\alpha - s_2) + C_2(r\dot{\phi}_2 \sin\alpha - \dot{s}_2), \tag{9}$$

$$\text{horizontal component}: \quad K_3(s_1 - r\phi_2) + C_3(\dot{s}_1 - r\dot{\phi}_2). \tag{10}$$

Substituting Eqs. (6)–(10) into Eqs. (2)–(4), the equations of motion are rewritten as follows:

$$\begin{aligned} m_1\ddot{s}_1 = {} & \{P + m_2 g + K_2(r\phi_1 \sin\alpha - s_2)\} + C_2(r\dot{\phi}_2 \sin\alpha - \dot{s}_2)\tan\alpha \\ & - \mu\{P + m_2 g + K_2(r\phi_2 \sin\alpha - s_2) + C_2(r\dot{\phi}_2 \sin\alpha - \dot{s}_2)\} \\ & - K_1 s_1 - K_3(s_1 - r\phi_2) - C_3(\dot{s}_1 - r\dot{\phi}_2), \end{aligned} \tag{11}$$

$$m_2\ddot{s}_2 = K_2(r\phi_2 \sin\alpha - s_2) + C_2(r\dot{\phi}_2 \sin\alpha - \dot{s}_2), \tag{12}$$

$$\begin{aligned}\frac{I_2}{r}\ddot{\phi}_2 = {} & \mu\{P + m_2 g + K_2(r\phi_2 \sin\alpha - s_2) + C_2(r\dot{\phi}_2 \sin\alpha - \dot{s}_2)\}\cos\alpha \\ & - \{P + m_2 g + K_2(r\phi_2 \sin\alpha - s_2) + C_2(r\dot{\phi}_2 \sin\alpha - \dot{s}_2)\}\sin\alpha \\ & + \{K_3(s_1 - r\phi_2) + C_3(\dot{s}_1 - r\dot{\phi}_2)\}\cos\alpha.\end{aligned} \tag{13}$$

6. Numerical simulation

In the numerical simulations, the Runge–Kutta method is employed to solve the equations of motion. The system parameters are shown in Table 4, where K_1 corresponds to the spring constant of the chain. Since this value is not indicated in the catalog, tension examination of the chain is performed. The linear approximation of the obtained characteristic is carried out within the experimental conditions, and the derived value is used. Next, the spring constant of material is described. First, for the perpendicular spring constant, the approximation formula of the compressive characteristic of the materials shown in Chapter 4 is used. For the horizontal spring constant, the Janssen theory [10], currently used for the design of tanks for powder, is used. That is, when materials are compressed, the horizontally generated pressure P_h is proportional to the perpendicular pressure P_v, and the proportionality constant is expressed with the following formula using the internal friction angle ϕ of materials.

$$\frac{P_h}{P_v} = K, \quad K = \frac{1 - \sin\phi}{1 + \sin\phi}. \tag{14}$$

Therefore, for the spring constant, K_3 is carried out by K times of K_2. The value of K used in this analysis is shown in Table 5.

On the other hand, it is difficult to identify the damping coefficient experimentally. Therefore, the damping coefficient of materials are given by the trial-and-error method. The value of C_2, C_3 used in this analysis are shown in Table 6.

It is considered that the friction characteristics of the materials between the table and the roller are decided by the relative velocity of the table to the roller. In this analysis, piecewise linear approximation shown in Fig. 27 is performed. As for the friction characteristics, the results obtained by the experiment of the simplified test apparatus are used. In respect of the relative velocity 0, it is usually supposed that the friction coefficient is changed from positive to negative instantly. However, the modeling of the friction characteristic considering this phenomenon includes a very strong discontinuity, and the direct numerical computation is difficult to

Table 4
List of parameters of the test apparatus

Mass of table	m_1	91.8 kg
Mass of roller	m_2	95.7 kg
Inertia of roller	I_2	0.9473 kg m^2
Radius of roller	r	0.15 m
Initial height of material	H	0.009 m
Spring constant of chain	K_1	7.329×10^5 N/m

Table 5
Horizontal spring constant of material

Material	ϕ: internal friction angle (deg)	K: proportionality constant (—)
Coarse	4.574	0.852
Fine	5.824	0.816

Table 6
Damping coefficient of material

Material	C_2: damping coefficient (Ns/m)	C_3: damping coefficient (Ns/m)
	Vertical direction	Horizontal direction
Coarse	1.25×10^2	3.00×10^4
Fine	1.25×10^2	4.00×10^4

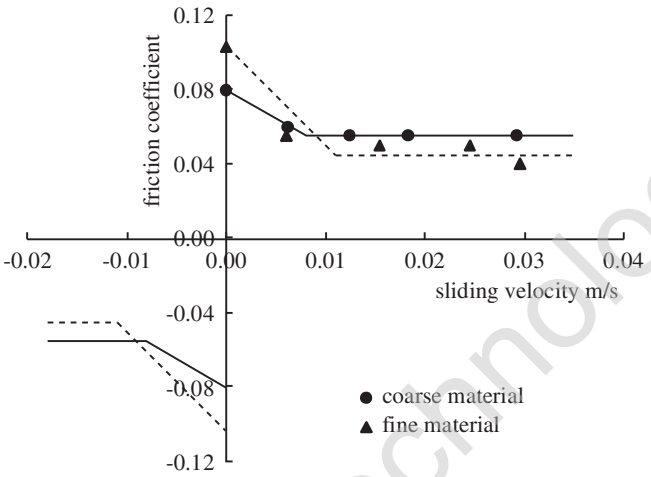

Fig. 27. Friction characteristics.

carry out. Therefore, the friction characteristics around the relative velocity zero are approximated by the straight line with a steep slope crossing the zero position.

As a simulation result, the response waveforms in the cases of the fine material and the coarse material are shown in Figs. 28 and 29 respectively. It is confirmed that similar fluctuation to the experimental results, which have a self-excited form, has occurred in the angular velocity of the roller and the tension force of the table. Moreover, the frequency of this fluctuation agrees well with that observed in the experiment. The frequency of this fluctuation coincides with the natural frequency which is calculated from the notation of the spring constant of chain K_1, the mass of table m_1 and the equivalent mass of roller m_3 ($= I_2/r^2$).

$$\omega = \frac{1}{2\pi}\sqrt{\frac{K_1}{m_1 + m_3}} = 11.8\,\text{Hz}.$$

This result agrees very well with the mill vibration characteristics. Furthermore, concerning the sliding velocity between the table and the roller, a similar stick–slip motion has occurred. And its fluctuation amplitude, when the particle size is fine, is larger than when the particle size is coarse. It is considered that the reason is that the negative slope of friction coefficient over the sliding velocity becomes significant when the material becomes finer. This result also corresponds qualitatively well with the feature that mill vibration occurs in the finer grinding conditions to produce material with fine particle size.

7. Conclusion

In this study, experimental analysis is performed for the purpose of clarifying the cause of the mill vibration. From the obtained characteristics of the mill vibration, it is denoted that the materials have a negative-damping property relative to the table speed in the fundamental experiment concerning friction characteristics. Further, a vibration model, considering the friction characteristics, is suggested. And by the numerical

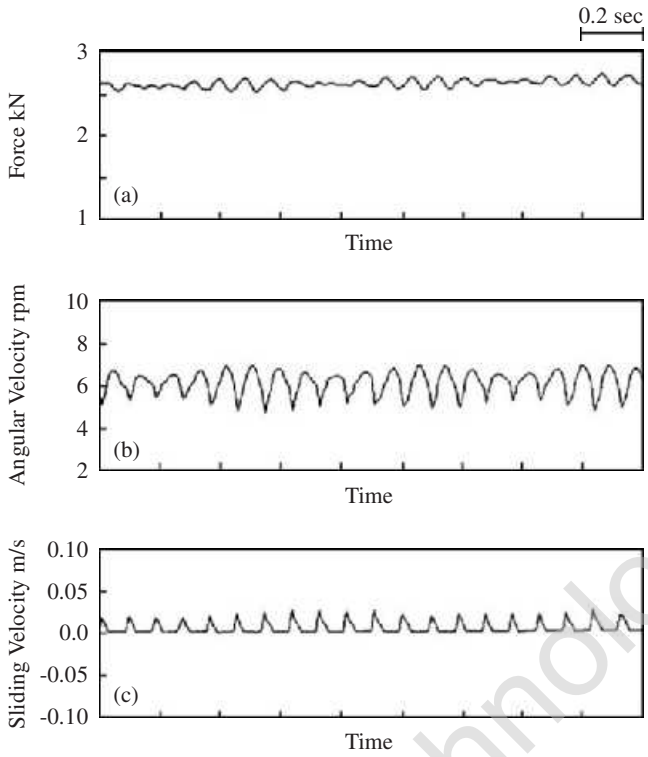

Fig. 28. Simulation results: (a) tension force of the table; (b) angular velocity of the roller; and (c) sliding velocity between the table and the roller when material is coarse.

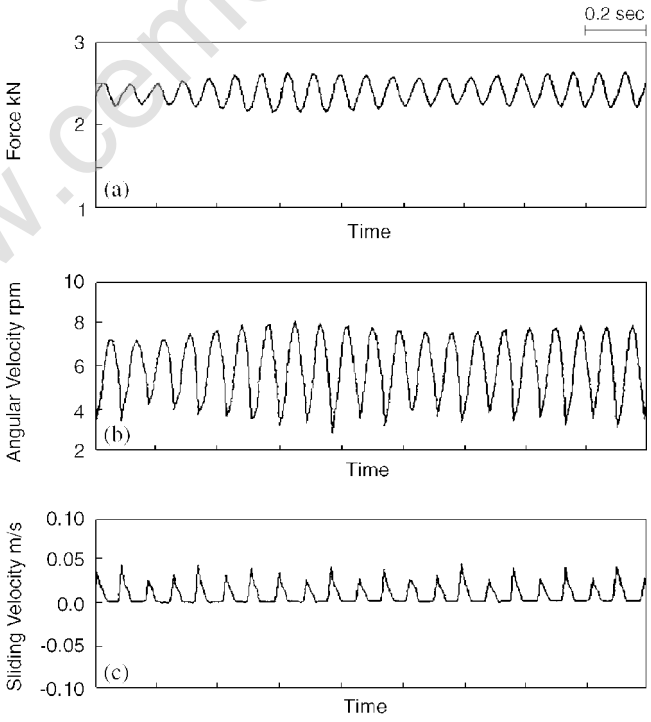

Fig. 29. Simulation results: (a) tension force of the table; (b) angular velocity of the roller; and (c) sliding velocity between the table and the roller when material is fine.

simulations of the vibration model, it is proved that the mill vibration is caused by the friction characteristics. The following results have been obtained:

1. The mill vibration is influenced by the behavior of the roller assembly, and the rotational motion of the roller fluctuates with the same frequency as the mill vibration frequency.
2. By the modal analysis for the roller supporting structure and the torsional driving system, it is found that mill vibration frequency is coincident with the first natural frequency of the torsional driving system and the mill vibration is due to the natural frequency of the torsional driving system.
3. The frictional coefficient of the materials tends to decrease according to the increase in the table speed. Its tendency becomes marked in fine materials and the amount of friction reduction from the static state to the dynamic state becomes large.
4. The vibration model of three-degrees-of-freedom with the obtained friction characteristics for a simplified test apparatus is proposed and the equations of motion are derived. Fluctuations similar to the experimental results are obtained by their numerical integration. It is confirmed that the fluctuation in the rotational motion of the roller is a stick–slip motion caused by the friction characteristics of materials.
5. Mill vibration is considered to be the result of the stick–slip motion of the rollers caused by the friction force between the table and the rollers, and this phenomenon is inherent to the material's negative-damping frictional property relative to the sliding velocity.

References

[1] E.J. Klovers, Energy savings with roller mills, *Zement-Kalk-Gips* 32 (1979) 24–29.
[2] P. Tiggesbaeumker, O. Knobloch, Finish grinding in the roller mill-developments and prospects, *Zement-Kalk-Gips* 32 (1979) 166–170.
[3] T. Ishikawa, T. Koga, H. Nomura, Raw material grinding equipment (UBE Loesche Mill), *Transactions of the JSIM* (1982) 10–13.
[4] L.T. Schneider, L. Lohnher, G. Gudat, Roller mills for high capacities and difficult material, *Zement-Kalk-Gips* 38 (1985) 705–708.
[5] K. Kaneko, Z. Morita, Characteristics and recent usage of vertical roller (ball) mills, *Powder Science and Engineering* 26 (4) (1994) 51–59.
[6] T. Ishikiwa, Foundation of Grinding Technology, *Plang and Process* (1994) 28–33.
[7] M. Inoue, Stick-slip motion of disk brake pads, *Transactions of the JSME C* 56 (521) (1990) 166–171.
[8] R. Suzuki, K. Yasuda, Analysis of chatter vibration in an automotive wiper assembly, *Transactions of the JSME C* 59 (559) (1993) 658–664.
[9] E. Takano, Y. Ohya, M. Saeki, Oscilations caused by solid friction in a hydraulic driving system, *Transactions of the JSMEC* 57 (540) (1991) 2539–2547.
[10] R.M. Nedderman, *Statics and Kinematics of Granular Materials*, Cambridge University Press, Cambridge, 1992.